ACS SyntheticBiology

pubs.acs.org/synthbio

Research Article

Reprogramming Gene Expression by Targeting RNA-Based Interactions: A Novel Pipeline Utilizing RNA Array Technology

Charlotte A. Henderson, Helen A. Vincent,* and Anastasia J. Callaghan*

Cite This: *ACS Synth. Biol.* 2021, 10, 1847−1858

Read Online

ACCESS | Metrics & More | Article Recommendations | Supporting Information

ABSTRACT: Regulatory RNA-based interactions are critical for coordinating gene expression and are increasingly being targeted in synthetic biology, antimicrobial, and therapeutic fields. Bacterial *trans*-encoded small RNAs (sRNAs) regulate the translation and/or stability of mRNA targets through base-pairing interactions. These interactions are often integral to complex gene circuits which coordinate critical bacterial processes. The ability to predictably modulate these gene circuits has potential for reprogramming gene expression for synthetic biology and antibacterial purposes. Here, we present a novel pipeline for targeting such RNA-based interactions with antisense oligonucleotides (ASOs) in order to reprogram gene expression. As proof-of-concept, we selected sRNA−mRNA interactions that are central to the *Vibrio cholerae* quorum sensing pathway, required for *V. cholerae* pathogenesis, as a regulatory RNA-based interaction input. We rationally designed anti-sRNA ASOs to target the sRNAs and synthesized them as peptide nucleic acids (PNAs). Next, we devised an RNA array-based interaction assay to allow screening of the anti-sRNA ASOs *in vitro*. Finally, an *Escherichia coli*-based gene expression reporter assay was developed and used to validate anti-sRNA ASO regulatory activity in a cellular environment. The output from the pipeline was an anti-sRNA ASO that targets sRNAs to inhibit sRNA−mRNA interactions and modulate gene expression. This anti-sRNA ASO has potential for reprogramming gene expression for synthetic biology and/or antibacterial purposes. We anticipate that this pipeline will find widespread use in fields targeting RNA-based interactions as modulators of gene expression.

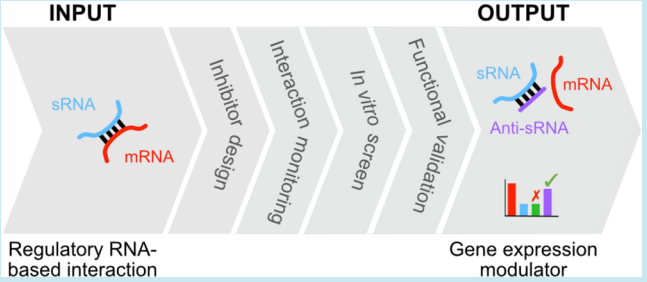

KEYWORDS: *antisense oligonucleotide (ASO), peptide nucleic acid (PNA), reprogramming gene expression, RNA array, RNA−RNA interactions, small regulatory RNA (sRNA)*

INTRODUCTION

RNA-based interactions, between noncoding RNAs and proteins, RNAs, and/or DNA, are essential for coordinating gene expression.[1] These regulatory interactions are increasingly being targeted in antimicrobial, therapeutic, and synthetic biology applications.[2−5] Bacteria contain on the order of hundreds of noncoding regulatory RNAs with the most abundant class being the *trans*-encoded small RNAs (sRNAs). sRNAs bind to mRNA targets through short, imperfect, base-pairing interactions. This results in the modulation of translation, and/or stability of the mRNA target(s), by affecting ribosome binding site (RBS) accessibility, or susceptibility to ribonucleases, respectively.[6,7] Individual sRNAs are typically integrated into complex gene circuits in which multiple sRNAs target multiple mRNAs to collectively control gene expression programs using a variety of regulatory strategies.[8] For example, sRNA-controlled gene circuits are often employed to regulate aspects of bacterial pathogenesis.[9,10] Therefore, the ability to predictably modulate these gene circuits has potential with regard to reprogramming gene expression for both synthetic biology and antibacterial purposes.

Since sRNA−mRNA base-pairing interactions are the basis of sRNA-regulated gene circuits, the obvious choice for a synthetic modulator would be an antisense oligonucleotide (ASO). ASOs are short, single-stranded oligonucleotides that bind to a complementary RNA target to affect its function.[11−13] Their sequence dependence means that they can be rationally designed to target any RNA of interest. Targeting mRNAs with ASOs is the strategy that is typically employed in the RNA therapeutics[12] and antibacterial[11,13] ASO fields. In the case of sRNA−mRNA interactions, an ASO that targets the mRNA (an anti-mRNA ASO) would effectively mimic the sRNA, leading to the formation of anti-mRNA

Received: November 30, 2020
Published: July 20, 2021

https://doi.org/10.1021/acssynbio.0c00603
ACS Synth. Biol. 2021, 10, 1847−1858

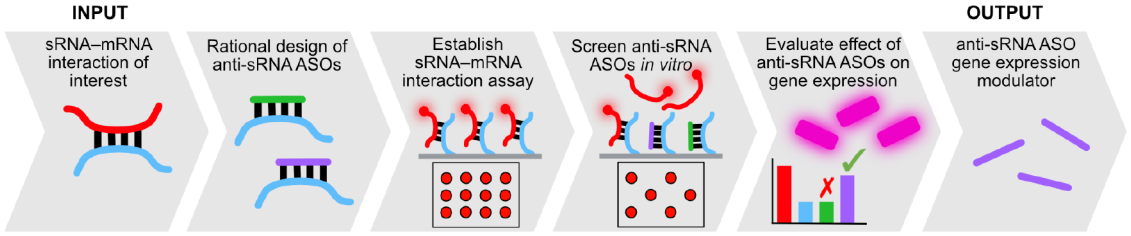

Figure 1. A pipeline for the production of anti-sRNA ASOs to reprogram gene expression. The input is an sRNA−mRNA interaction of interest. Anti-sRNA ASOs are rationally designed to target the sRNA. An *in vitro* sRNA−mRNA interaction assay is established. The anti-sRNA ASOs are screened in the *in vitro* sRNA−mRNA interaction assay. Promising anti-sRNA ASOs are evaluated in a gene expression assay. The output anti-sRNA ASO gene expression modulator can be taken forward for future applications, e.g., integration into synthetic gene circuits or the development of antibacterial ASOs.

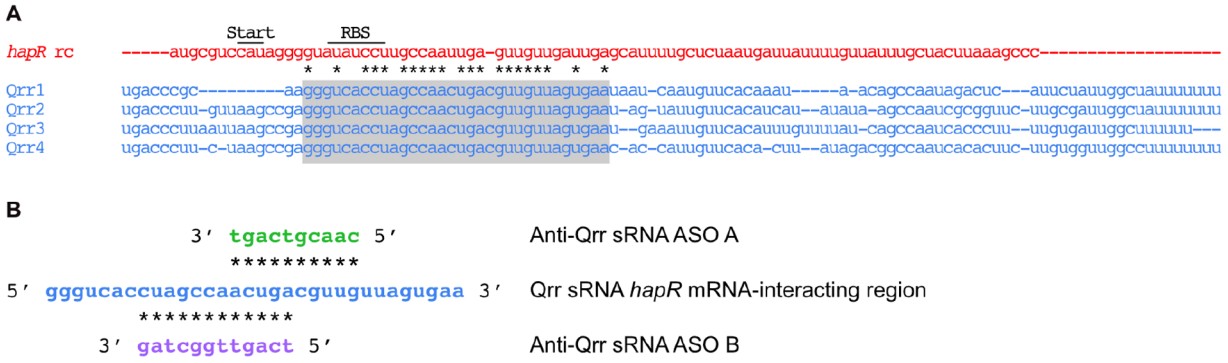

Figure 2. Rational design of anti-Qrr sRNA ASOs. (A) A multiple sequence alignment of the reverse complement of *V. cholerae hapR* mRNA (−80 to +10; red, *hapR* rc) and Qrr sRNAs (blue, Qrr1−4). The RNA sequences were extracted from Lenz et al.[18] and aligned in Clustal Omega.[24] The alignment was edited manually based on Lenz et al.[18] The locations of the ribosome binding site (RBS) and start codon (Start) within the *hapR* rc sequence are indicated. The 32-nucleotide *hapR*-interacting region,[18] within the Qrr sRNAs, is highlighted with a gray box. Identity between the Qrr sRNAs and the *hapR* rc sequence, representing nucleotides which mediate the Qrr sRNA−*hapR* mRNA interactions, is indicated by asterisks. (B) The sequences of the anti-Qrr sRNA ASOs (green, Anti-Qrr sRNA ASO A; purple, Anti-Qrr sRNA ASO B) and their target binding sites within the *hapR* mRNA-interacting region of the Qrr sRNAs (blue). Asterisks indicate the expected base-pairing interactions between the anti-Qrr sRNA ASOs and the Qrr sRNAs.

ASO−mRNA interactions, blocking the formation of sRNA−mRNA interactions. In contrast, an anti-sRNA ASO, that mimics the mRNA target and sequesters the sRNA would inhibit sRNA activity to prevent the sRNA−mRNA interaction. Indeed, there are examples of endogenous "sponge RNAs"[14] and synthetic anti-miRNAs[3] that utilize this mechanism of target mimicry. Both strategies have merit; however, here we have focused on expanding existing two-component sRNA/mRNA systems to three-component sRNA/mRNA/anti-sRNA systems.

We decided to target the sRNA−mRNA interactions that are central to the quorum sensing system of the human pathogen *Vibrio cholerae* (see Supporting Figure S1 for a simplified schematic). *V. cholerae* utilizes an sRNA-regulated gene circuit to orchestrate group behaviors, including host colonization and virulence factor production, in response to cell density.[15−17] At low cell density, during the early stages of infection, four functionally redundant quorum regulatory sRNAs (Qrr1−4) are expressed.[18,19] The Qrr sRNAs target a number of mRNAs, including *hapR* mRNA, which encodes the master regulator HapR.[18−21] Base-pairing between the Qrr sRNAs and the 5′ untranslated region (UTR) of *hapR* mRNA is facilitated by Hfq and represses *hapR*.[18−21] *hapR* repression is one key factor that ultimately results in a gene expression profile that promotes host colonization and virulence factor production. Conversely, at high cell density, during the late stages of infection, the Qrr sRNAs are no longer expressed. In the absence of the Qrr sRNAs, *hapR* expression is activated, and this promotes a gene expression profile that favors release of the bacterium from the host, ready for the infection cycle to begin again. Sequestering the Qrr sRNAs with an anti-Qrr sRNA ASO, and thereby preventing Qrr sRNA−*hapR* mRNA interactions, would be expected to reprogram the gene circuit, locking it into the high cell density expression profile, which could have antibacterial implications.

In the current work, we developed a pipeline for generating anti-sRNA ASOs to reprogram gene expression (Figure 1) and demonstrated its application to *V. cholerae* quorum sensing sRNA−mRNA interactions. The input for the pipeline was the *V. cholerae* Qrr sRNA−*hapR* mRNA interactions. We rationally designed two anti-Qrr sRNA ASOs to target the Qrr sRNAs and inhibit the Qrr sRNA−*hapR* mRNA interactions. These were synthesized as peptide nucleic acids (PNAs), a synthetic DNA mimic with a neutral backbone[22] (Supporting Figure S2A). An *in vitro* Qrr sRNA−*hapR* mRNA interaction assay, based on our innovative RNA array technology,[23] was established to monitor the sRNA−mRNA interactions. The anti-Qrr sRNA ASOs were screened, using this assay, for the ability to inhibit the Qrr sRNA−*hapR* mRNA interactions. Both anti-Qrr sRNA ASOs inhibited the Qrr sRNA−*hapR* mRNA interactions. Finally, a Qrr1/*hapR*−mCherry gene expression reporter assay was developed in *Escherichia coli* to test the ability of the anti-Qrr sRNA ASOs to reprogram gene expression in a cellular environment. One anti-Qrr sRNA ASO

https://doi.org/10.1021/acssynbio.0c00603
ACS Synth. Biol. 2021, 10, 1847−1858

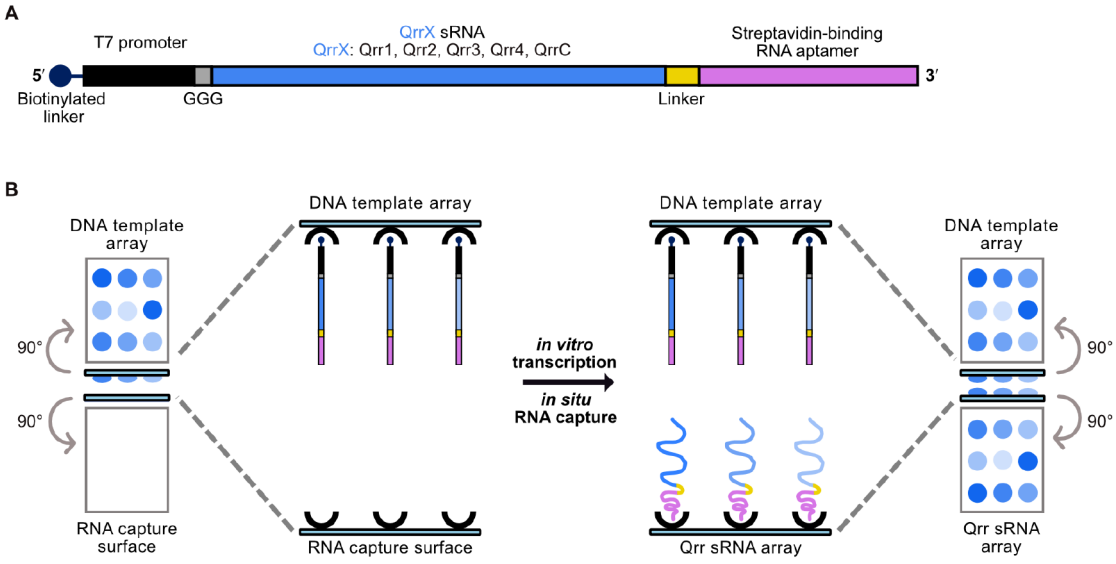

Figure 3. Generating a Qrr sRNA array. (A) A schematic showing the general architecture of the DNA *in vitro* transcription templates. From 5′ to 3′ each double-stranded DNA template consists of a 5′ biotinylated linker, a T7 promoter, a GGG trinucleotide repeat, a sequence encoding the Qrr sRNA (QrrX), a sequence encoding a linker, and a sequence encoding a streptavidin-binding RNA aptamer. *In vitro* transcription templates were designed for Qrr1−4 sRNAs and a control Qrr sRNA, QrrC, which is Qrr1 with a scrambled *hapR* mRNA-interacting region. The sequences of the *in vitro* transcription templates can be found in Supporting Table S1. (B) A schematic of the "sandwich" method,[23] involving *in vitro* transcription and *in situ* RNA capture, that was used to generate the Qrr sRNA arrays. A DNA template array—*in vitro* transcription reagent solution—streptavidin-coated RNA capture slide "sandwich" was assembled. Qrr sRNAs were synthesized by *in vitro* transcription and captured *in situ* on a streptavidin-coated RNA capture surface, via their streptavidin-binding RNA aptamer affinity tag. The result is an sRNA array.

successfully derepressed the Qrr1/*hapR*−mCherry reporter system, validating it as a synthetic gene expression modulator. Therefore, the output from the pipeline was an anti-Qrr sRNA ASO that can inhibit Qrr sRNA−*hapR* mRNA interactions and modulate gene expression. This anti-sRNA ASO has potential for reprogramming gene expression for synthetic biology and/or antibacterial purposes.

RESULTS AND DISCUSSION

Rational Design of Anti-Qrr sRNA ASOs. The first stage of the pipeline to produce anti-sRNA ASOs to modulate gene expression is to design anti-Qrr sRNA ASOs to target the Qrr sRNAs and inhibit the Qrr sRNA−*hapR* mRNA interactions. To do this, we needed to both identify a target site within the Qrr sRNAs and select an appropriate chemistry for ASO synthesis. *V. cholerae* contains four Qrr sRNAs (Qrr1−4) which each contain an identical 32-nucleotide region that interacts with the 5′ UTR of *hapR* mRNA to block the RBS and inhibit translation[18] (Figure 2A). Therefore, this was the obvious region to target with anti-Qrr sRNA ASOs. Furthermore, because this region is identical in each Qrr sRNA, an anti-Qrr sRNA ASO targeting this region should target all four Qrr sRNAs.

With regard to ASO chemistry, we ruled out using unmodified DNA or RNA because early attempts to use natural oligonucleotide ASOs had limited success due to their susceptibility to cellular nucleases and the challenges of poor cellular uptake.[11−13] Chemical advances in the ASO field have resulted in a number of synthetic nucleic acid analogues that have improved resistance to nucleases, enhanced binding specificity, and enhanced binding kinetics.[12,13] Those most commonly employed for bacterial applications include PNAs and phosphorodiamidate morpholinos (PMOs).[11,13] We decided to use PNAs for our anti-Qrr sRNA ASOs due to the accessibility of custom PNA synthesis. The optimal length for PNA ASOs has been found to be 10 to 12 nucleotides.[25,26] Considering this parameter, two ASO sequences, one 10 nucleotides in length and one 12 nucleotides in length, were designed to target the core *hapR*-interacting region within the Qrr sRNAs (Figure 2B). These anti-Qrr sRNA ASO sequences were synthesized as fluorophore−cell-penetrating peptide (CPP)−PNA conjugates (Supporting Figure S2B and C).

Development of an *In Vitro* Interaction Assay to Monitor Qrr sRNA−*hapR* mRNA Interactions. Having rationally designed anti-Qrr sRNA ASOs, we needed to develop an *in vitro* Qrr sRNA−*hapR* mRNA interaction assay in which to screen them. We recently developed an innovative "sandwich" method for the production of functional-RNA arrays, involving *in vitro* transcription of a DNA template array and *in situ* RNA capture on a facing surface.[23] These RNA arrays can be used as a platform for investigating multiple RNA-based interactions, including sRNA−mRNA interactions, in parallel.[23,27,28] Consequently, we decided to use this technology to generate a Qrr sRNA array, to be used as the basis for a Qrr sRNA−*hapR* mRNA interaction assay (Figure 3).

To generate a Qrr sRNA array, we first needed to design *in vitro* transcription DNA templates encoding the Qrr sRNAs. Double-stranded *in vitro* transcription templates all had the general architecture shown in Figure 3A.[23] The Qrr sRNAs that are transcribed from these templates will be Qrr sRNA−linker−streptavidin-binding RNA aptamer conjugates. Briefly, a 5′-biotinylated linker facilitates immobilization on a streptavidin-coated surface. This is followed by a T7 promoter and a GGG trinucleotide repeat. The GGG sequence ensures that there is a G in the +1, +2, and +3 positions, as required for optimal T7 RNA polymerase activity.[29] Next is the sequence encoding the Qrr sRNA (QrrX) followed by a sequence

https://doi.org/10.1021/acssynbio.0c00603
ACS Synth. Biol. 2021, 10, 1847−1858

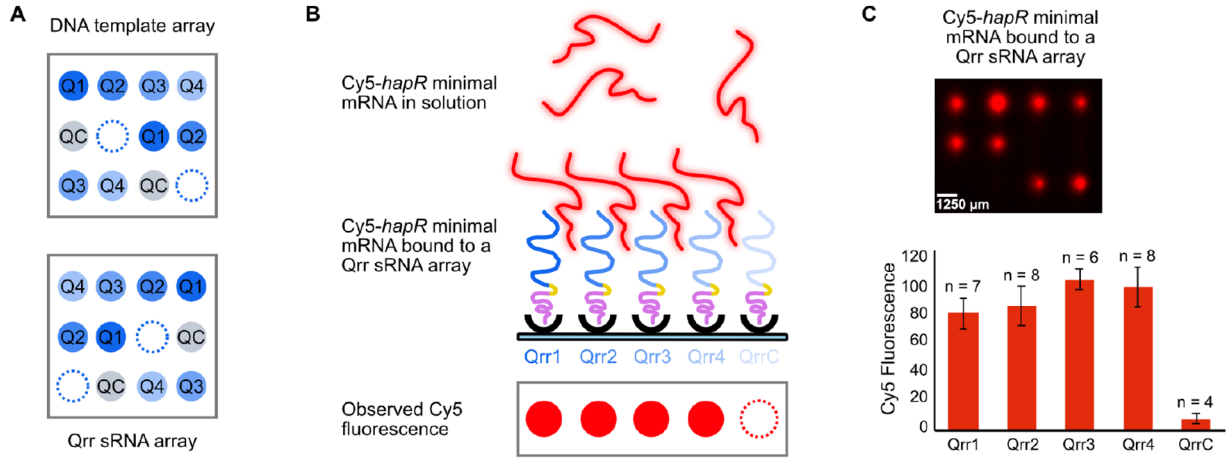

Figure 4. An *in vitro* Qrr sRNA−*hapR* mRNA interaction assay. (A, upper panel) A schematic layout of a 4 × 3 field of the Qrr sRNA DNA template array (Qrr1, Q1; Qrr2, Q2; Qrr3, Q3; Qrr4, Q4; QrrC, QC). No DNA was spotted at the positions indicated by dashed circles. (A, lower panel) A schematic layout of a 4 × 3 field of the expected Qrr sRNA array. No RNA was expected to be captured at the positions indicated by dashed circles. Note that the layout of the Qrr sRNA array is the mirror image of the DNA template array. (B) A schematic of Cy5-*hapR* minimal mRNA applied to a Qrr sRNA array in solution. Cy5-*hapR* minimal mRNA is expected to bind to Qrr1−4 sRNAs to establish Qrr sRNA−*hapR* mRNA interactions. Cy5-*hapR* minimal mRNA is not expected to bind to QrrC. The Cy5 fluorescence that would be expected to be observed on the sRNA array is also shown schematically. (C, upper panel) A representative 4 × 3 field of a Qrr sRNA array, following the application of Cy5-*hapR* minimal mRNA, visualized for Cy5 fluorescence (the array layout is as shown in A, lower panel). (C, lower panel) A bar chart of the normalized mean Cy5 fluorescence observed for Qrr1, Qrr2, Qrr3, Qrr4, and QrrC sRNAs when Cy5-*hapR* minimal mRNA was applied to the Qrr sRNA array. The Cy5 fluorescence at each array position was normalized to the Dy649 fluorescence observed at the same array position when Dy649-RNA linker probe was applied to the same Qrr sRNA array, following a wash step to remove bound Cy5-*hapR* minimal mRNA (Supporting Figure S3). The mean fluorescence intensity for each Qrr sRNA has been normalized to the highest mean fluorescence intensity (Qrr3 sRNA). Error bars represent the standard deviation.

encoding a short linker sequence and, finally, a sequence encoding a streptavidin-binding RNA aptamer. The linker aims to promote the independent folding of the Qrr sRNA and the streptavidin-binding RNA aptamer, and it also provides a binding site for a fluorescently labeled DNA oligonucleotide probe, enabling quantification of the relative levels of Qrr sRNA on the generated array.[27,28] The 3′ streptavidin-binding RNA aptamer acts as an affinity tag to facilitate *in situ* surface capture of the RNA. *In vitro* transcription templates were designed for all four Qrr sRNAs (Qrr1−4) and a control Qrr sRNA (QrrC) which is Qrr1 with a scrambled *hapR* mRNA-interacting region (see Supporting Table S1 for sequences). QrrC should not interact with *hapR* mRNA and should not be targeted by the anti-Qrr sRNA ASOs.

We then set out to generate a Qrr sRNA array using our "sandwich" method (Figure 3B).[23] 5′-Biotinylated *in vitro* transcription templates for Qrr1−4 and QrrC were assembled by gene synthesis and PCR. These were spotted onto a streptavidin-coated DNA capture surface (a glass microarray slide), in an array format, using an automated arrayer (Figure 4A, upper panel). A DNA template array—*in vitro* transcription reagent solution—RNA capture surface (a streptavidin-coated glass microarray slide) "sandwich" was then assembled (Figure 3B). As *in vitro* transcription proceeded, the Qrr sRNAs were captured *in situ*, via their streptavidin-binding RNA aptamer affinity tag, as an RNA array on the RNA capture surface (Figure 3B and Figure 4A, lower panel). The 3′ location of the streptavidin-binding RNA aptamer affinity tag ensured that only fully transcribed, full-length RNA transcripts, with a correctly folded streptavidin-binding RNA aptamer, were captured to generate the sRNA array.

Once the Qrr sRNA array had been produced, Qrr sRNA−*hapR* mRNA interactions needed to be established on the array. This required the cognate *hapR* mRNA. Since the known sequence and structural elements required for the Qrr sRNAs to bind to *hapR* mRNA are contained entirely within the 5′ UTR of the *hapR* mRNA,[18−21] a minimal *hapR* mRNA molecule consisting of the complete 5′ UTR and 10 nucleotides of the protein-coding region was designed to contain these elements. We have previously shown that this region of *hapR* mRNA is sufficient to facilitate the *V. cholerae* Qrr1 sRNA−*hapR* mRNA interaction on an RNA array.[23] An *in vitro* transcription template encoding the *hapR* minimal mRNA was designed, and this was generated by gene synthesis. Internally, Cy5-labeled *hapR* minimal mRNA (Cy5-*hapR* minimal mRNA) was produced by supplementing a standard *in vitro* transcription reaction with Cy5-UTP. When a solution of Cy5-*hapR* minimal mRNA is added to a Qrr sRNA array, it would be expected to interact with Qrr1−4 sRNAs to establish Qrr sRNA−*hapR* mRNA interactions on the array, but it would not be expected to interact with QrrC, which lacks a functional *hapR* mRNA-interacting region (Figure 4B). A solution of Cy5-*hapR* minimal mRNA was added to the Qrr sRNA array, and the array was visualized under conditions to detect Cy5 fluorescence. Cy5 fluorescence was clearly detected at the array positions containing Qrr1, Qrr2, Qrr3, and Qrr4 sRNAs, indicating that Cy5-*hapR* minimal mRNA had bound to these sRNAs to establish Qrr sRNA−*hapR* mRNA interactions (Figure 4C, upper panel). As expected, no Cy5 fluorescence could be detected at the positions containing QrrC, suggesting that Cy5-*hapR* minimal mRNA does not bind to QrrC (Figure 4C, upper panel).

As can be seen in Figure 4C, upper panel, the observed Cy5 fluorescence, representing the Qrr sRNA−*hapR* mRNA interactions, was variable. This could be due to variable amounts of Qrr sRNA being present at each position of the

https://doi.org/10.1021/acssynbio.0c00603
ACS Synth. Biol. 2021, 10, 1847−1858

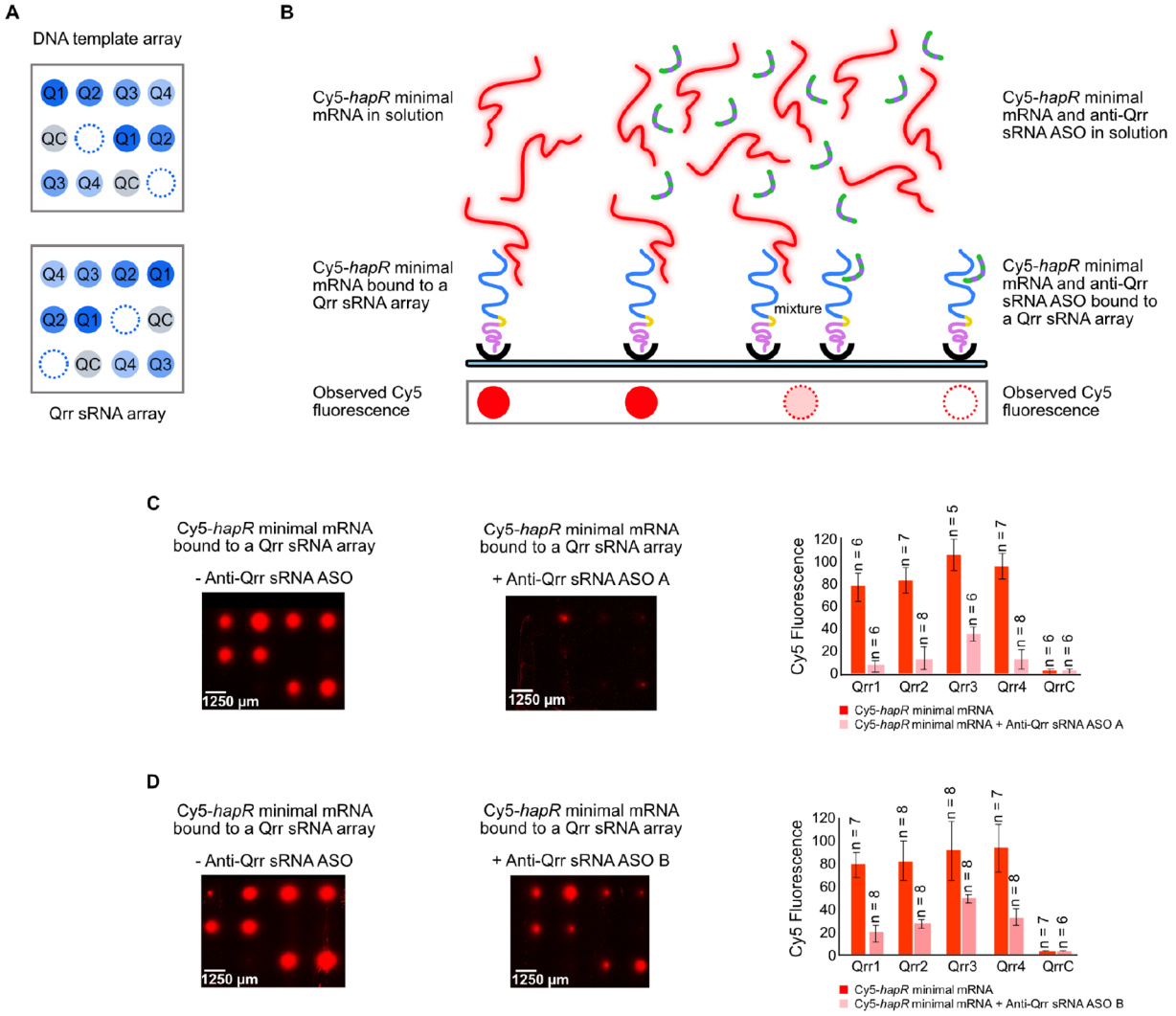

Figure 5. Evaluating anti-Qrr sRNA ASO activity *in vitro*. (A) A schematic layout of a 4 × 3 field of the Qrr sRNA DNA template array and a 4 × 3 field of the Qrr sRNA array, as described in the legend to Figure 4. (B) A schematic showing the expected outcomes when a solution of either Cy5-*hapR* minimal mRNA alone, or a mixture of Cy5-*hapR* minimal mRNA and anti-Qrr sRNA ASO, is applied to a Qrr sRNA array (see the main text for further description). (C and D, left panels) A representative 4 × 3 field of a Qrr sRNA array, following the application of Cy5-*hapR* minimal mRNA, visualized for Cy5 fluorescence (the array layout is as shown in A, lower panel). (C and D, middle panels) A representative 4 × 3 field of a Qrr sRNA array, following the application of a mixture of Cy5-*hapR* minimal mRNA and anti-Qrr sRNA ASO (C, Anti-Qrr sRNA ASO A; D, Anti-Qrr sRNA ASO B), visualized for Cy5 fluorescence (the array layout is as shown in A, lower panel). (C and D, right panels) A bar chart of the normalized mean Cy5 fluorescence observed for Qrr1, Qrr2, Qrr3, Qrr4, and QrrC sRNAs when Cy5-*hapR* minimal mRNA (red bars) and a mixture of Cy5-*hapR* minimal mRNA and anti-Qrr sRNA ASO (pink bars; C, Anti-Qrr sRNA ASO A; D, Anti-Qrr sRNA ASO B), was applied to the Qrr sRNA array. The Cy5 fluorescence at each array position was normalized to the Dy649 fluorescence observed at the same array position when Dy649-RNA linker probe was applied to the same Qrr sRNA arrays, following a wash step to remove bound Cy5-*hapR* minimal mRNA (Supporting Figure S5). The mean fluorescence intensity for each Qrr sRNA has been normalized to the highest mean fluorescence intensity. Error bars represent the standard deviation.

Qrr sRNA array, depending upon the combined efficiency of RNA synthesis and capture at that position. To control for varying transcription/capture efficiencies, we decided to determine the relative amount of Qrr sRNA present at each array position and normalize the observed Cy5 fluorescence to this value. To this end, we designed a 5′ Dy649-labeled single-stranded 20-mer DNA oligonucleotide, complementary to the common linker region between the Qrr sRNA and the streptavidin-binding RNA aptamer (Dy649-RNA linker probe). When a solution of Dy649-RNA linker probe is added to a Qrr sRNA array, it would be expected to interact with Qrr1−4 sRNA and QrrC sRNA (Supporting Figure S3A). We have previously utilized fluorescently labeled complementary DNA oligonucleotides to probe the relative amount of RNA present at individual positions of an RNA array.[27,28] Given that the Cy5-*hapR* minimal mRNA and Dy649-RNA linker probe are expected to bind to different regions of the Qrr sRNAs, it is unlikely that binding of one would affect binding of the other. However, Cy5-*hapR* minimal mRNA can also be efficiently removed from the Qrr sRNA during a wash step, prior to the addition of Dy649-RNA linker probe (Supporting Figure S4A). Since similar results were obtained with Dy649-RNA linker probe regardless of whether or not the array had been previously exposed to Cy5-*hapR* minimal mRNA (Supporting Figure S4), we elected to first expose the Qrr sRNA array to Cy5-*hapR* minimal mRNA, then remove

https://doi.org/10.1021/acssynbio.0c00603
ACS Synth. Biol. 2021, 10, 1847−1858

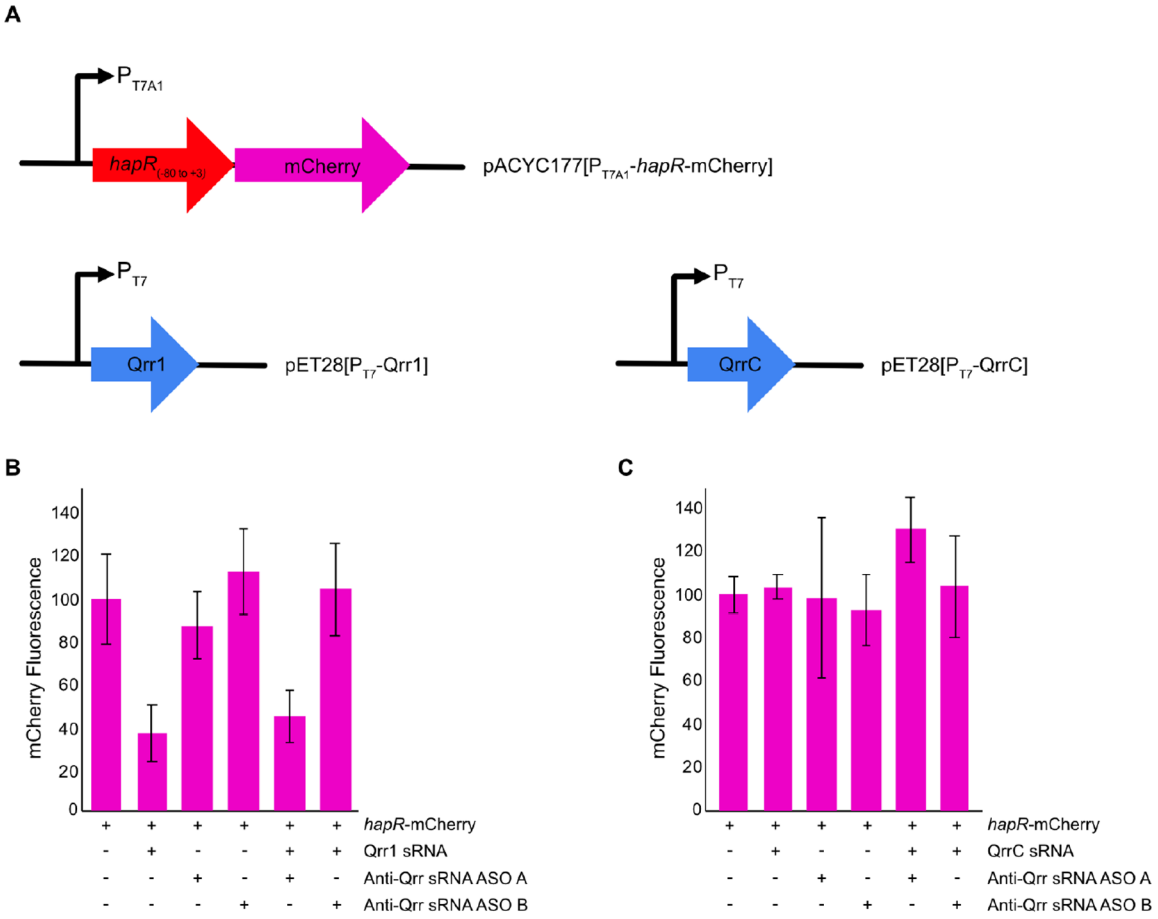

Figure 6. Evaluating anti-Qrr sRNA ASO activity in a gene expression assay. (A) A schematic representation of the *hapR*-mCherry, Qrr1, and QrrC expression plasmids (see Supporting Table S3 for sequence information). *hapR*-mCherry is expressed from the constitutive T7A1 promoter. Qrr1 and QrrC expression is induced with IPTG using the pET system. (B and C) Bar charts showing the relative mCherry fluorescence observed in the presence of the indicated system components. Data are the mean of three experimental repeats, and error bars represent the standard deviation.

the bound Cy5-*hapR* minimal mRNA with a wash step, and finally probe with Dy649-RNA linker probe.

The *hapR* minimal mRNA-bound Qrr sRNA array (Figure 4C, upper panel) was washed, to remove the bound Cy5-*hapR* minimal mRNA, probed with Dy649-RNA linker probe, and visualized for Dy649 fluorescence (Supporting Figure S3B and C). Dy649 fluorescence was detected at the array positions containing Qrr1, Qrr2, Qrr3, Qrr4, and QrrC sRNAs, indicating that Dy649-RNA linker probe had bound to all five Qrr sRNAs and, critically, that all five Qrr sRNAs had been efficiently synthesized and captured (Supporting Figure S3C, upper panel). Detection of QrrC, using Dy649-RNA linker probe, supports the conclusion that the lack of Cy5 fluorescence observed at the QrrC positions is due to the expected lack of Cy5-*hapR* minimal mRNA binding, and not due to failure of the RNA transcription/capture procedure. The relative levels of each Qrr sRNA did vary (Supporting Figure S3C, lower panel), indicating that the Qrr sRNAs are synthesized/captured with different efficiencies. It is not clear why the transcription/capture efficiencies vary, but it does highlight the need to factor in the captured RNA levels on the array, when analyzing data. When the Cy5 fluorescence intensity, corresponding to bound Cy5-*hapR* minimal mRNA, was normalized to the Dy649 fluorescence, to adjust for the Qrr sRNA level, it appears that a similar fraction of Qrr1, Qrr2, Qrr3, and Qrr4 sRNA is bound by Cy5-*hapR* minimal mRNA (Figure 4C, lower panel).

Evaluation of Anti-Qrr sRNA ASO Activity *In Vitro*. Having rationally designed anti-Qrr sRNA ASOs, and established an *in vitro* assay to monitor the Qrr sRNA–*hapR* mRNA interactions, the next step was to screen the anti-Qrr sRNA ASOs for the ability to target the Qrr sRNAs and inhibit the sRNA–*hapR* mRNA interactions. A Qrr sRNA array of Qrr1–4 and QrrC sRNAs was generated (Figure 5A), as described above. Parallel experiments were then performed in which a solution of either Cy5-*hapR* minimal mRNA alone, or a mixture of Cy5-*hapR* minimal mRNA and anti-Qrr sRNA ASO, was applied to the Qrr sRNA array. In the absence of anti-Qrr sRNA ASO, Cy5-*hapR* minimal mRNA would be expected to bind to sRNAs Qrr1–4 (Figure 5B, left). In the presence of anti-Qrr sRNA ASO, three outcomes are possible (Figure 5B, right). First, Cy5-*hapR* minimal mRNA may completely outcompete the anti-Qrr sRNA ASO to bind to the Qrr sRNAs, which would result in an observed Cy5 fluorescence level similar to that observed in the absence of anti-Qrr sRNA ASO. Second, Cy5-*hapR* minimal mRNA may partially outcompete the anti-Qrr sRNA ASO such that some Qrr sRNA molecules will be bound by Cy5-*hapR* minimal mRNA and others will be bound by anti-Qrr sRNA ASO. In this case, the observed Cy5 fluorescence would be reduced compared to that observed in the absence of anti-Qrr sRNA

https://doi.org/10.1021/acssynbio.0c00603
ACS Synth. Biol. 2021, 10, 1847–1858

ASO. Finally, the anti-Qrr sRNA ASO could completely outcompete Cy5-*hapR* minimal mRNA, which would result in no Cy5 fluorescence being observed.

As observed previously (Figure 4C), when Cy5-*hapR* minimal mRNA was applied to the Qrr sRNA in the absence of anti-Qrr sRNA ASO, Cy5 fluorescence was detected at the array positions containing Qrr1, Qrr2, Qrr3, and Qrr4 sRNAs but not at the array positions containing the negative control sRNA QrrC (Figure 5C and D, left panels). When a mixture of Cy5-*hapR* minimal mRNA and anti-Qrr sRNA ASO was added to the Qrr sRNA array, Cy5 fluorescence could still be detected at the positions containing Qrr1, Qrr2, Qrr3 and Qrr4 sRNAs; however, the Cy5 fluorescence levels were much lower than those observed in the absence of anti-Qrr sRNA ASO (Figure 5C and D, middle panels). This effect was greater for Anti-Qrr sRNA ASO A than it was for Anti-Qrr sRNA B. To confirm that the reduction in Cy5 fluorescence, representing bound Cy5-*hapR* minimal mRNA, was most likely due to the anti-Qrr sRNA ASOs binding to the Qrr sRNAs and outcompeting the Cy5-*hapR* minimal mRNA and not due to variable Qrr sRNA levels on the array, the relative RNA levels were quantified using Dy649-RNA linker probe. The *hapR* minimal mRNA-bound Qrr sRNA arrays (Figure 5C and D, left and middle panels) were washed, to remove the bound Cy5-*hapR* minimal mRNA, probed with Dy649-RNA linker probe and visualized for Dy649 fluorescence (Supporting Figure S5). When the Cy5 fluorescence was normalized to the Dy649 fluorescence, it is clear that the anti-Qrr sRNA ASOs inhibit Cy-5 *hapR* minimal mRNA binding to the Qrr sRNAs (Figure 5C and D, right panels). Since each of the anti-Qrr sRNA ASOs had been synthesized as a Cy3 conjugate (Supporting Figure S2B and C), simultaneous monitoring of both Cy5-*hapR* minimal mRNA and anti-Qrr sRNA ASO binding was possible. The same Qrr sRNA arrays shown in Figure 5C and D, middle panels, were visualized for Cy3 fluorescence (Supporting Figure S6). Cy3 fluorescence, representing bound anti-Qrr sRNA ASO, was detected at the array positions containing Qrr1, Qrr2, Qrr3, and Qrr4 sRNAs but not at the array positions containing QrrC, as expected (Supporting Figure S6). Taken together, these data suggest that both Anti-Qrr sRNA ASO A and Anti-Qrr sRNA ASO B bind to Qrr1−4 sRNAs and partially outcompete Cy5-*hapR* minimal mRNA to inhibit the Qrr sRNA−*hapR* mRNA interactions.

Evaluation of Anti-Qrr sRNA ASO Activity in a Gene Expression Assay. Having ascertained that the anti-Qrr sRNA ASOs are able to bind to the Qrr sRNAs and inhibit the Qrr sRNA−*hapR* mRNA interactions *in vitro*, we next wanted to test if this would be translated into a change in gene expression in a cellular environment. To do this, we elected to design a gene expression reporter assay that could be carried out in *E. coli*. *E. coli* has been used previously to test Qrr sRNA activity because it is both a "lab safe" organism and it does not possess a quorum sensing system of its own, allowing direct effects of exogenous Qrr sRNAs to be assessed (e.g., Bardill and Hammer[30]). We designed a two-plasmid reporter system to test the effects of the anti-Qrr sRNA ASOs on Qrr1 (Figure 6A). One plasmid was a low-copy number plasmid that expressed a *hapR* (−80 to +3)-mCherry transcriptional fusion from the constitutive T7A1 promoter (pACYC177[P_{T7A1}-*hapR*-mCherry]). The second was a medium-copy number pET plasmid that, upon induction with IPTG, expressed either Qrr1 sRNA (pET28[P_{T7}-Qrr1]) or the control QrrC sRNA (pET28[P_{T7}-QrrC]). In the absence of IPTG, *hapR*-mCherry was constitutively expressed, and mCherry fluorescence was high (Figure 6B and C, first bars). Upon addition of IPTG, the expression of Qrr1, or QrrC, sRNA was induced. Induction of Qrr1 sRNA resulted in repression of *hapR*-mCherry and a reduction in mCherry fluorescence (Figure 6B, compare first and second bars). This can be explained if, as expected, Qrr1 sRNA binds to *hapR*-mCherry mRNA, blocking the RBS, and inhibiting translation. In contrast, induction of QrrC sRNA, which is not expected to bind to *hapR*-mCherry, did not repress *hapR*-mCherry or lead to a reduction in the observed mCherry fluorescence (Figure 6C, compare first and second bars).

We next wanted to test the effect of the anti-Qrr sRNA ASOs on mCherry fluorescence, both in the absence of Qrr sRNAs and in the presence of either Qrr1 sRNA or QrrC sRNA. Cellular uptake of "naked" PNA by *E. coli* is known to be inefficient.[11−13] This can be improved by conjugating the PNA to a cell-penetrating peptide (CPP).[13] Good et al. have demonstrated that uptake of PNAs by *E. coli* can be facilitated through the conjugation of the CPP $(KFF)_3K$ to the PNA.[25] It was for this reason that our anti-Qrr sRNA ASOs were synthesized with this CPP conjugated to the PNA ASO (Supporting Figure S2B and C). In the absence of Qrr sRNAs, neither anti-Qrr sRNA ASO affected mCherry fluorescence (Figure 6B and C, compare first, third, and fourth bars). In the presence of both Qrr1 sRNA and Anti-Qrr sRNA ASO A, the observed mCherry fluorescence was similar to that observed in the presence of Qrr1 sRNA alone (Figure 6B, compare second and fifth bars). However, in the presence of both Qrr1 and Anti-Qrr sRNA ASO B, *hapR*-mChery was derepressed and the observed mCherry fluorescence was restored to that observed in the absence of Qrr1 (Figure 6B, compare first and sixth bars). In the presence of QrrC, which does not repress *hapR*-mCherry and affect mCherry fluorescence, addition of anti-Qrr sRNA ASO also did not affect mCherry fluorescence (Figure 6C, compare, first, second, fifth, and sixth bars). These results suggest that Anti-Qrr sRNA ASO B successfully targets Qrr1 sRNA to modulate *hapR*-mCherry expression in a cellular environment.

The lack of activity of Anti-Qrr sRNA ASO A in the gene expression assay was surprising given the results from the *in vitro* interaction assay (Figure 5). There are several possibilities for this result, including an insufficient intracellular concentration of Anti-Qrr sRNA ASO A to outcompete *hapR*-mCherry mRNA for Qrr1 binding. This could be due to poor cellular uptake and/or sequestration of Anti-Qrr sRNA ASO A. We had attempted to mitigate the risk of poor cellular uptake by conjugating the anti-Qrr sRNA ASOs to a CPP (Supporting Figure S2B and C), and this strategy appears to have been successful for Anti-Qrr sRNA ASO B. Since the anti-Qrr sRNA ASOs were Cy3-labeled, we used confocal microscopy to visualize the mCherry and Cy3 fluorescence in *E. coli* cells expressing *hapR*-mCherry in the presence of Anti-Qrr sRNA ASO A (Supporting Figure S7). The fluorescence from mCherry did appear to coincide with the Cy3 fluorescence from Anti-Qrr sRNA ASO A, indicating that the anti-Qrr sRNA ASO is entering the cells. As *E. coli* does take up Anti-Qrr sRNA ASO A, a possibility is that it is sequestered by binding to an endogenous RNA. Off-target effects are known to be a common problem with ASOs, in part due to their relatively short length failing to provide the required specificity in a cellular context.[12,26] The specificity of the longer 12-

https://doi.org/10.1021/acssynbio.0c00603
ACS Synth. Biol. 2021, 10, 1847−1858

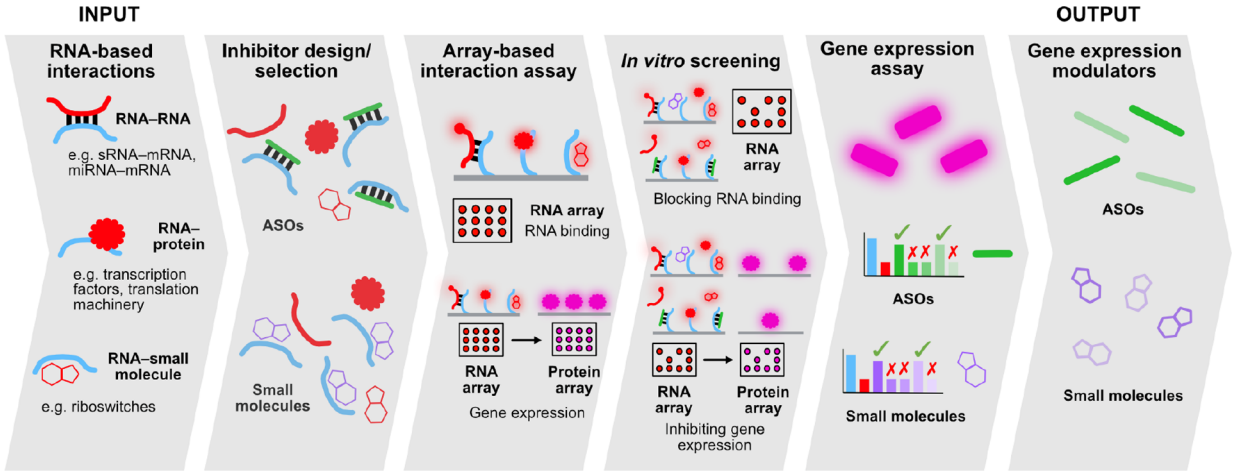

Figure 7. A pipeline for the production of modulators of gene expression. The input for the pipeline is a regulatory RNA-based interaction involved in gene expression. Candidate inhibitors, which could be ASOs or small molecules, are rationally designed, or selected for screening, to target the RNA-based interaction. A simple *in vitro* binding assay, using functional-RNA array technology,[23] is then established. This can be extended to monitor the gene expression output on a reporter-protein array.[27] Candidate inhibitors are screened using the simple *in vitro* assay(s). Their ability to modulate gene expression is validated in a cellular environment. The outputs from the pipeline are gene expression modulators that can be taken forward in the development of synthetic biology, antibacterial, or therapeutic strategies.

nucleotide Anti-Qrr sRNA ASO B may be enhanced relative to 10-nucleotide Anti-Qrr ASO A.

An Anti-Qrr sRNA ASO Inhibitor of Qrr sRNA–*hapR* mRNA Binding Interactions Which Modulates Gene Expression. We have successfully developed a pipeline for the production of anti-sRNA ASOs and used it to produce an anti-Qrr sRNA ASO (Anti-Qrr sRNA ASO B) that both inhibits Qrr sRNA–*hapR* minimal mRNA binding interactions *in vitro* and modulates gene expression in a Qrr1 sRNA/*hapR*-mCherry reporter system, in *E. coli*. This effectively expands an existing two-component gene expression system to a three-component gene expression system. Although we have focused on the individual Qrr sRNA–*hapR* mRNA interactions, this could be expanded further to incorporate all four Qrr sRNAs, *hapR* mRNA, and Anti-Qrr sRNA ASO B. Likewise, although we evaluated gene expression using a reporter system in *E. coli*, it is anticipated that this would be readily transferrable to cell-free expression systems.

The Qrr sRNA–*hapR* mRNA interactions are central to the quorum sensing system that coordinates the infection cycle of *V. cholerae*[15−17] (Supporting Figure S1). The Qrr sRNA–*hapR* mRNA interactions are required during the early stages of *V. cholerae* infection to establish a gene expression profile which promotes virulence (Supporting Figure S1). However, the lack of Qrr sRNA expression at the late stages of infection results in the absence of Qrr sRNA–*hapR* mRNA interactions and promotes release of *V. cholerae* from its host (Supporting Figure S1). Due to the link between quorum sensing systems and pathogenesis, quorum sensing has been identified as a process with potential for antibacterial targeting.[31,32] Inhibition of the Qrr sRNA–*hapR* mRNA interactions, by Anti-Qrr sRNA ASO B, would be expected to effectively mimic the situation at high cell density when there are no Qrr sRNAs present, and this might be expected to prevent host colonization and virulence factor production. Therefore, Anti-Qrr sRNA ASO B also has potential as a lead compound for antibacterial targeting of *V. cholerae* through the reprogramming of gene expression.

A Pipeline for Targeting RNA-Based Interactions to Modulate Gene Expression. Although we have applied our pipeline to a very specific bacterial RNA-based interaction, there is enormous scope to expand its applicability (Figure 7). The input for the pipeline can be essentially any regulatory RNA-based interaction involved in gene expression, including RNA–RNA interactions, RNA–protein interactions, and RNA–small molecule interactions. These interactions may be targeted for synthetic biology, antimicrobial, and/or therapeutic purposes. For example, target RNA–RNA interactions could be bacterial sRNA–mRNA interactions, such as the Qrr sRNA–*hapR* interactions, or the analogous eukaryotic micro RNA (miRNA)–mRNA interactions.[33] Increasing numbers of miRNAs are being identified as attractive therapeutic targets due to their role(s) in human diseases such as cancer, cardiovascular disease, and diabetes.[3] Or, it may be desirable to target the RNA–protein interactions involved in the transcription and translation processes or the RNA–small molecule interactions central to the action of bacterial riboswitches.[34]

The first stage of the pipeline is to select candidate inhibitors to target the RNA-based interaction. Candidate inhibitors can be rationally designed, or could be screening libraries. For RNA–RNA interactions, assuming that the sequence of the RNA-binding partners is known, it is relatively straightforward to rationally design ASOs to target the interacting region of one, or both, of the RNAs. As we have demonstrated here for the Qrr sRNAs and *hapR* mRNA, this approach may only require the design of a handful of candidate ASO inhibitors. ASOs could also be designed to target known protein-binding, or small molecule-binding, sites within an RNA, although this information is often less readily available. Alternatively, there is precedent for targeting RNA with small molecules, e.g., riboswitches[34] and antimicrobial aminoglycosides that target 16S rRNA.[35] The rational design of small molecule inhibitors is far more challenging than ASO design and often, a screening library of hundreds, or thousands, of small molecules is likely to be a suitable starting point in this case. Having selected candidate inhibitors, the next step of the pipeline is to establish

https://doi.org/10.1021/acssynbio.0c00603
ACS Synth. Biol. 2021, 10, 1847−1858

a simple *in vitro* assay, to monitor the RNA-based interaction, that can be used for inhibitor screening. Regardless of whether the input is an RNA−RNA, RNA−protein, or RNA−small molecule interaction, a simple binding assay can be used to monitor the interaction. We elected to use functional-RNA arrays[23] as the basis for the RNA−RNA Qrr sRNA−*hapR* mRNA binding interactions. Although other interaction methodologies could be employed, e.g., surface plasmon resonance (SPR)[36] or electrophoretic mobility shift assays (EMSAs), an advantage of using RNA array technology is its high-throughput capacity. This capacity can be used to perform multiple experimental repeats in parallel on a single RNA array, for a small number of related interactions, as we have done here for the four Qrr sRNA−*hapR* mRNA interactions. Alternatively, it can be used to monitor multiple orthogonal RNA-based interactions simultaneously,[23] limited only by the availability of orthogonal detection methods. Furthermore, although a binding assay would be expected to be predictive of the gene expression outcome, this can be directly assessed by taking the RNA array-based binding assay and using it, in turn, to generate a reporter-protein array.[27] This provides a cell-free gene expression readout. Having established a suitable *in vitro* assay, the candidate inhibitors are then screened in order to identify inhibitors with potential to modulate gene expression. Both of the anti-Qrr sRNA ASOs that we had rationally designed inhibited the Qrr sRNA−*hapR* mRNA interactions in a binding assay and were taken forward for testing in a more complex assay. More complex assays are likely to validate modulation of gene expression in a cellular environment, which may encounter the possible challenges of cellular uptake and/or off-target effects. Our results highlight the importance of including this validation step since only Anti-Qrr sRNA ASO B modulated the expression of a *hapR*-mCherry reporter in a three-component Qrr1 sRNA/*hapR*-mCherry mRNA/Anti-Qrr sRNA ASO B system. The output from the pipeline is a modulator of gene expression that targets an RNA-based interaction. This could be deployed as a switch in a synthetic biology context. For example, the Qrr1 sRNA/*hapR*-mCherry mRNA/Anti-Qrr sRNA ASO B system could be integrated into synthetic gene circuits, or adapted to control other pathways. Alternatively, if the RNA-based interactions are of interest from an antibacterial or therapeutic perspective, as is the case for the Qrr sRNA−*hapR* mRNA interactions, the inhibitor/modulator could be taken forward as a lead compound in an antibacterial or therapeutic strategy.

CONCLUDING REMARKS

In conclusion, we have developed a pipeline to produce inhibitors of regulatory RNA-based interactions which can be used as modulators of gene expression. We designed two anti-Qrr sRNA ASOs to target the *V. cholerae* Qrr sRNAs, inhibit the Qrr sRNA−*hapR* mRNA interactions, and thereby regulate *hapR* expression. A simple RNA array-based Qrr sRNA−*hapR* mRNA interaction assay was designed to screen the anti-Qrr sRNA ASOs for the ability to inhibit the Qrr sRNA−*hapR* mRNA interaction, demonstrating the potential to modulate gene expression of a two component Qrr sRNA/*hapR* mRNA system. Both anti-Qrr sRNA ASOs were able to outcompete *hapR* mRNA in this interaction assay. We went on to show that one of the anti-Qrr sRNA ASOs (Anti-Qrr sRNA ASO B) derepresses a Qrr sRNA/*hapR* mRNA reporter system in a cellular environment. We anticipate that this gene expression modulator will be of use as a synthetic biology component and/or a lead molecule for antibacterial targeting of *V. cholerae*. Furthermore, we hope that the broader pipeline will find widespread use in the identification of inhibitors of RNA-based interactions to reprogram gene expression for synthetic biology, antimicrobial, and/or therapeutic applications.

METHODS

Anti-Qrr sRNA ASO Design and Synthesis. Anti-sRNA ASO sequences were designed to target the Qrr sRNAs using the PNA design tool PNABio and the default restraints (Anti-Qrr sRNA ASO A: 5′-caa cgt cag t-3′; Anti-Qrr sRNA ASO B: 5′-tca gtt gc tag-3′). The anti-Qrr sRNA ASOs were synthesized as Cy3−CPP−PNA conjugates (see Supporting Figure S2B and C) by Panagene.

Production of Qrr sRNA Arrays. *Design and Preparation of In Vitro Transcription Templates for DNA Template Arrays.* Double-stranded DNA *in vitro* transcription templates encoding Qrr sRNA−linker−streptavidin-binding RNA aptamer conjugates were designed essentially as described in Phillips et al.[23] (see Figure 3A and Results and Discussion for details). Their sequences are presented in Supporting Table S1. Core templates, lacking the 5′-biotinylated linker, were initially assembled by gene synthesis (see Supporting Table S2 for the primer sequences). These were amplified in a standard PCR reaction using the forward primer 5′-biotin-ctc gag taa tac gac tca cta tag g-3′ and the relevant antisense 2 primer from Supporting Table S2 as the reverse primer. The resulting biotinylated double-stranded DNA *in vitro* templates were purified using a NucleoSpin gel and PCR cleanup kit (Macherey-Nagel). Their concentrations were determined by measuring the A_{260}, and their size was confirmed by agarose gel electrophoresis.

Preparation of Streptavidin-Coated DNA and RNA Capture Surfaces. Streptavidin-coated surfaces were prepared as described in Phillips et al.[23] Briefly, NHS-activated Nexterion H microarray slides (Schott) were coated with 90 μL 1 μM or 90 μL 16.7 μM streptavidin in phosphate-buffered saline (PBS) at pH 7.4, for the preparation of DNA or RNA capture surfaces, respectively. Coated slides were covered with a 24 × 60 mm LifterSlip (Thermo Fisher Scientific) and incubated at 37 °C for 1 h in a humidified chamber. The LifterSlips were removed, and the slides were washed at room temperature with 45 mL of PBS and 0.05% (v/v) Tween 20 (PBS-T) for 5 min with rolling, followed by 45 mL of PBS for 5 min with rolling, followed by 45 mL of H_2O for 5 min with rolling (wash-cycle A). To block any unreacted NHS functional groups, the slides were then submerged in 45 mL of 50 mM ethanolamine-HCl at pH 8.5 and incubated at room temperature for 30 min with rolling. The slides were washed at room temperature following wash-cycle A and then dried by centrifugation at 500*g* for 3 min at room temperature.

Preparation of DNA Template Arrays. A solution of each 5′-biotinylated *in vitro* transcription template was prepared at a concentration of 300 nM in PBS. These solutions were spotted onto a streptavidin-coated DNA capture surface in 4 × 3 fields, at a spot separation of 2500 μm, using an automated arrayer (Genetix Qarray2) fitted with a 200 μm pin head. Following spotting, the slides were incubated at 20 °C and 50% relative humidity for 30 min, washed at room temperature following wash-cycle A, and dried by centrifugation at 500*g* for 3 min at room temperature.

RNA Synthesis and In Situ Surface Capture. A DNA template array—*in vitro* transcription reagent solution (150 μL

https://doi.org/10.1021/acssynbio.0c00603
ACS Synth. Biol. 2021, 10, 1847−1858

1× Reaction Buffer (MEGAscript T7 Transcription Kit, Thermo Fisher Scientific), 1× Enzyme Mix (MEGAscript T7 Transcription Kit), and 0.5 mM of ATP, CTP, GTP, and UTP)—streptavidin-coated RNA capture surface "sandwich" was assembled, essentially as described in Phillips et al.[23] The sandwich assembly was incubated at 37 °C for 90 min in a humidified chamber to allow for *in vitro* transcription and *in situ* RNA capture. The DNA template array and the newly generated sRNA array were separated. The sRNA array was washed at room temperature following wash-cycle A and dried by centrifugation at 500*g* for 3 min at room temperature.

An *In Vitro* Qrr sRNA–*hapR* mRNA Interaction Assay. *Design and Synthesis of hapR Minimal mRNA.* A double-stranded DNA *in vitro* transcription template encoding *hapR* minimal mRNA (−80 to +10) was designed to contain all of the known sequence and structural elements required to bind the Qrr sRNAs[18−21] (see Supporting Table S1 for the sequence). RNA secondary structure predictions were utilized to guide the design process.[37−39] The double-stranded DNA *in vitro* transcription template was assembled by gene synthesis (see Supporting Table S2 for the primer sequences). It was purified using a NucleoSpin gel and PCR cleanup kit. Its concentration was determined by measuring the A_{260}, and its size was confirmed by agarose gel electrophoresis. Cy5-labeled *hapR* minimal mRNA was then synthesized by *in vitro* transcription using a MEGAscript T7 transcription kit (Thermo Fisher Scientific) supplemented with 0.05 mM Cy5-UTP (GE Healthcare Life Sciences). Cy5-*hapR* minimal mRNA was purified using a MEGAclear transcription cleanup kit (Thermo Fisher Scientific). The concentration was determined by measuring the A_{260}, and its size was confirmed by denaturing 7 M urea 10% polyacrylamide gel electrophoresis.

Hybridization of Cy5-hapR Minimal mRNA to Qrr sRNA Arrays. A 1 μM solution of Cy5-*hapR* minimal mRNA, or a mixture of 1 μM Cy5-*hapR* minimal mRNA and 1.5 μM anti-Qrr sRNA ASO, was prepared in hybridization buffer (40 mM Tris, pH 7.8; 6 mM $MgCl_2$; 20 mM NaCl), heated at 80 °C for 10 min and allowed to cool at room temperature for 10 min. A volume of 20 μL was then pipetted onto a Qrr sRNA array and covered with a 22 × 22 mm LifterSlip (CNTech). This assembly was incubated at 25 °C for 90 min in the dark. The LifterSlip was removed, and the Cy5-*hapR* minimal mRNA-bound Qrr sRNA array was washed at room temperature with 45 mL of hybridization buffer for 1 min with rolling, followed by 45 mL of H_2O for 10 s with rolling (wash-cycle B). The Cy5-*hapR* minimal mRNA-bound Qrr sRNA array was dried by centrifugation at 500*g* for 3 min at room temperature.

Visualization and Quantification of Cy5 Fluorescence. Cy5-*hapR* minimal mRNA, bound to a Qrr sRNA array, was visualized using a GenePix 4200A microarray slide scanner (Molecular Devices) with the following settings: excitation wavelength, 635 nm; power, 80; emission filter, Standard Red (676/29 nm); PMT gain, 550. The fluorescence intensity at each position of the array was quantified using GenePix software (Molecular Devices). To aid visualization, the images were false-colored red, and the brightness and contrast of the images were both set to 98 in the GenePix software. Brightness and contrast were further adjusted to 65 and 30, respectively, in PowerPoint.

Removal of Bound Cy5-hapR Minimal mRNA from Qrr sRNA Arrays. To remove bound Cy5-*hapR* minimal mRNA from Qrr sRNA arrays, 90 μL of 2× saline-sodium citrate (SSC) supplemented with 0.1% sodium dodecyl sulfate (SDS; w/v) was pipetted over a Qrr sRNA array and covered with a 24 × 60 mm LifterSlip. This assembly was incubated at room temperature for 30 min. The LifterSlip was removed, and the Qrr sRNA array was washed at room temperature with 45 mL of PBS-T for 5 min with rolling, followed by 45 mL of H_2O for 1 min with rolling, followed by a dip in 45 mL of H_2O (wash-cycle C). The Qrr sRNA array was dried by centrifugation at 500*g* for 3 min at room temperature.

Dy649-RNA Linker Probe Synthesis. A Dy649-labeled DNA oligonucleotide (5′-Dy649–gtg tgt gtg tgt gtg tgt gt-3′) complementary to the linker region between the Qrr sRNA and the streptavidin-binding RNA aptamer (Dy649-RNA linker probe) was obtained from Thermo Fisher Scientific.

Hybridization of Dy649-RNA Linker Probe to Qrr sRNA Arrays. A 100 nM solution of Dy649-RNA linker probe was prepared in 2× SSC supplemented with 0.1% SDS. A total of 90 μL was then pipetted onto a Qrr sRNA array and covered with a 24 × 60 mm LifterSlip. This assembly was incubated at 25 °C for 30 min in the dark. The LifterSlip was removed, and Dy649-RNA linker probe-bound Qrr sRNA array was washed at room temperature with 45 mL of PBS-T for 5 min with rolling, followed by 45 mL of H_2O for 1 min with rolling, followed by a dip in 45 mL of H_2O (wash-cycle D). The Dy649-RNA linker probe-bound Qrr sRNA array was dried by centrifugation at 500*g* for 3 min at room temperature.

Visualization and Quantification of Dy649 Fluorescence. Dy649-RNA linker probe, bound to a Qrr sRNA array, was visualized using a GenePix 4200A microarray slide scanner with the following settings: excitation wavelength, 635 nm; power, 80; emission filter, Standard Red (676/29 nm); PMT gain, 550. The fluorescence intensity at each position of the array was quantified using GenePix software. To aid visualization, the images were false-colored yellow, and the brightness and contrast of the images were both set to 98 in the GenePix software. Brightness and contrast were further adjusted to 65 and 30, respectively, in PowerPoint.

A Qrr/*hapR*-mCherry Gene Expression Assay. *Generation of the hapR-mCherry, Qrr1, and QrrC Expression Strains.* DNA sequence encoding P_{T7A1}-*hapR*-mCherry was synthesized and cloned into the *Nhe*I and *Hin*dIII restriction sites of the pACYC177 (Amp^R) vector by GeneArt (Thermo Fisher Scientific; see Supporting Table S3 for sequence information). DNA sequences encoding P_{T7}-Qrr1 and P_{T7}-QrrC were assembled by gene synthesis and cloned into the *Bgl*II and *Xho*I sites of pET28b (Kan^R; see Supporting Table S3 for sequence information). The sequences of the vectors were confirmed by DNA sequencing. The *E. coli* expression strain BL21(DE3) was cotransformed with pACYC177[P_{T7A1}-*hapR*-mCherry] and either pET28[P_{T7}-Qrr1] or pET28[P_{T7}-QrrC].

Qrr/hapR-mCherry Gene Expression Assay. BL21(DE3) pACYC177[P_{T7A1}-*hapR*-mCherry] pET28[P_{T7}-Qrr1] and BL21(DE3) pACYC177[P_{T7A1}-*hapR*-mCherry] pET28[P_{T7}-QrrC] were grown to single colonies on LB agar, supplemented with 100 μg/mL ampicillin and 50 μg/mL kanamycin, at 37 °C; 5 μL of resuspended cells was used to inoculate 125 μL of Mueller-Hinton (MH) broth, supplemented with 100 μg/mL of ampicillin, 50 μg/mL of kanamycin, 1% (w/v) glucose, either 0 or 200 μM IPTG, and either 0 or 3 μM Anti-Qrr sRNA ASO A or 0 or 1.5 μM Anti-Qrr sRNA ASO B. These cultures were incubated in black clear-bottomed 96-well plates (Corning), with orbital shaking,

https://doi.org/10.1021/acssynbio.0c00603
ACS Synth. Biol. 2021, 10, 1847−1858

at 37 °C, in a Hidex Sense plate reader. The OD_{600} and the mCherry fluorescence (excitation wavelength, 575 nm; emission wavelength, 616 nm) were recorded every 10 min for 3 h. The $(\text{fluorescence}_{OD(600)=0.6} - \text{fluorescence}_{OD(600)=0.2})/(\text{time}_{OD(600)=0.6} - \text{time}_{OD(600)=0.2})$ was calculated.

■ ASSOCIATED CONTENT

Supporting Information

The Supporting Information is available free of charge at https://pubs.acs.org/doi/10.1021/acssynbio.0c00603.

Methods for visualization of anti-Qrr sRNA ASOs bound to Qrr sRNA arrays and for visualization of mCherry and Anti-Qrr sRNA ASO A in *E. coli*; abbreviations; references; *in vitro* transcription template, primer, and plasmid insert, sequences used in this study (Supporting Tables S1−S3); schematic of *V. cholerae* quorum sensing (Supporting Figure S1); structure and sequences of the anti-Qrr sRNA ASOs used in this study (Supporting Figure S2); Dy649-RNA linker probe data for Qrr sRNA arrays (Supporting Figures S3−S5); anti-Qrr sRNA ASOs bound to Qrr sRNA arrays (Supporting Figure S6); confocal microscopy of mCherry and Anti-Qrr sRNA ASO A in *E. coli* (Supporting Figure S7) (PDF)

■ AUTHOR INFORMATION

Corresponding Authors

Helen A. Vincent − *School of Biological Sciences and Institute of Biological and Biomedical Sciences, University of Portsmouth, Portsmouth PO1 2DY, United Kingdom*; Email: Helen.Vincent@port.ac.uk

Anastasia J. Callaghan − *School of Biological Sciences and Institute of Biological and Biomedical Sciences, University of Portsmouth, Portsmouth PO1 2DY, United Kingdom*; orcid.org/0000-0003-4272-4835; Email: Anastasia.Callaghan@port.ac.uk

Author

Charlotte A. Henderson − *School of Biological Sciences and Institute of Biological and Biomedical Sciences, University of Portsmouth, Portsmouth PO1 2DY, United Kingdom*

Complete contact information is available at: https://pubs.acs.org/10.1021/acssynbio.0c00603

Author Contributions

All authors conceived ideas and devised methodology. C.A.H. carried out the experimental work and formal data analysis. All authors contributed to the interpretation of the data. C.A.H. and H.A.V. prepared the original draft. All authors critically reviewed, revised, and approved the final version of the manuscript. A.J.C. acquired the funding for the project.

Notes

The authors declare the following competing financial interest(s): A.J.C. is a named inventor on patents that relate to aspects of the work reported here. University of Portsmouth has been granted the following patents: US9777268B2 (US patent) and EP2732047B1 (European patent). C.A.H. and H.A.V. have no conflicts of interest to declare.

■ ACKNOWLEDGMENTS

We thank members of A.J.C.'s research group (University of Portsmouth, UK), between 2012 and 2021, for helpful discussions and technical support. We thank Dr. Jonathan Watts (University of Massachusetts Medical School, USA) for helpful discussions. We thank Dr. T.J. Ragan (University of Leicester, UK) for helpful discussions and critical reading of the manuscript. This work was supported by funding from the Biotechnology and Biological Sciences Research Council (BB/M020576/1 to A.J.C. and BB/I532988/1 to A.J.C.) and Research England E3 funding. Funding for the open access charge was from the Biotechnology and Biological Sciences Research Council.

■ ABBREVIATIONS

ASO, antisense oligonucleotide; CPP, cell-penetrating peptide; MH, Mueller-Hinton; PBS, phosphate-buffered saline; PBS-T, phosphate-buffered saline supplemented with 0.05% (v/v) Tween 20; PMO, phosphorodiamidate morpholino; PNA, peptide nucleic acid; Qrr sRNA, quorum regulatory small RNA; RBS, ribosome binding site; SDS, sodium dodecyl sulfate; sRNA, small RNA; SSC, saline-sodium citrate; UTR, untranslated region

■ REFERENCES

(1) Schönberger, B., Schaal, C., Schäfer, R., and Voß, B. (2018) RNA interactomics: recent advances and remaining challenges. *F1000Research 7*, 1824.

(2) Dersch, P., Khan, M. A., Mühlen, S., and Görke, B. (2017) Roles of regulatory RNAs for antibiotic resistance in bacteria and their potential value as novel drug targets. *Front. Microbiol. 8*, 803.

(3) Rupaimoole, R., and Slack, F. J. (2017) MicroRNA therapeutics: towards a new era for the management of cancer and other diseases. *Nat. Rev. Drug Discovery 16*, 203−222.

(4) Villa, J. K., Su, Y., Contreras, L. M., and Hammond, M. C. (2018) Synthetic biology of small RNAs and riboswitches, *Microbiol. Spectrum 6*, DOI: 10.1128/microbiolspec.RWR-0007-2017.

(5) Apura, P., Domingues, S., Viegas, S. C., and Arraiano, C. M. (2019) Reprogramming bacteria with RNA regulators. *Biochem. Soc. Trans. 47*, 1279−1289.

(6) Waters, L. S., and Storz, G. (2009) Regulatory RNAs in bacteria. *Cell 136*, 615−628.

(7) Storz, G., Vogel, J., and Wassarman, K. M. (2011) Regulation by small RNAs in bacteria: expanding frontiers. *Mol. Cell 43*, 880−891.

(8) Beisel, C. L., and Storz, G. (2010) Base pairing small RNAs and their roles in global regulatory networks. *FEMS Microbiol. Rev. 34*, 866−882.

(9) Svensson, S. L., and Sharma, C. M. (2016) Small RNAs in bacterial virulence and communication, *Microbiol. Spectrum 4*, DOI: 10.1128/microbiolspec.VMBF-0028-2015.

(10) Westermann, A. J. (2018) Regulatory RNAs in virulence and host-microbe interactions, *Microbiol. Spectrum 6*, DOI: 10.1128/microbiolspec.RWR-0002-2017.

(11) Sully, E. K., and Geller, B. L. (2016) Antisense antimicrobial therapeutics. *Curr. Opin. Microbiol. 33*, 47−55.

(12) Khvorova, A., and Watts, J. K. (2017) The chemical evolution of oligonucleotide therapies of clinical utility. *Nat. Biotechnol. 35*, 238−248.

(13) Hegarty, J. P., and Stewart, D. B., Sr (2018) Advances in therapeutic bacterial antisense biotechnology. *Appl. Microbiol. Biotechnol. 102*, 1055−1065.

(14) Denham, E. L. (2020) The sponge RNAs of bacteria - how to find them and their role in regulating the post-transcriptional network. *Biochim. Biophys. Acta, Gene Regul. Mech. 1863*, 194565.

(15) Ng, W. L., and Bassler, B. L. (2009) Bacterial quorum-sensing network architectures. *Annu. Rev. Genet. 43*, 197−222.

(16) Ball, A. S., Chaparian, R. R., and van Kessel, J. C. (2017) Quorum sensing gene regulation by LuxR/HapR master regulators in *Vibrios*. *J. Bacteriol. 199*, e00105−17.
(17) Pérez-Reytor, D., Plaza, N., Espejo, R. T., Navarrete, P., Bastías, R., and Garcia, K. (2017) Role of non-coding regulatory RNA in the virulence of human pathogenic *Vibrios*. *Front. Microbiol. 7*, 2160.
(18) Lenz, D. H., Mok, K. C., Lilley, B. N., Kulkarni, R. V., Wingreen, N. S., and Bassler, B. L. (2004) The small RNA chaperone Hfq and multiple small RNAs control quorum sensing in *Vibrio harveyi* and *Vibrio cholerae*. *Cell 118*, 69−82.
(19) Svenningsen, S. L., Tu, K. C., and Bassler, B. L. (2009) Gene dosage compensation calibrates four regulatory RNAs to control *Vibrio cholerae* quorum sensing. *EMBO J. 28*, 429−439.
(20) Rutherford, S. T., van Kessel, J. C., Shao, Y., and Bassler, B. L. (2011) AphA and LuxR/HapR reciprocally control quorum sensing in *vibrios*. *Genes Dev. 25*, 397−408.
(21) Shao, Y., and Bassler, B. L. (2012) Quorum-sensing non-coding small RNAs use unique pairing regions to differentially control mRNA targets. *Mol. Microbiol. 83*, 599−611.
(22) Nielsen, P. E., Egholm, M., Berg, R. H., and Buchardt, O. (1991) Sequence-selective recognition of DNA by strand displacement with a thymine-substituted polyamide. *Science 254*, 1497−1500.
(23) Phillips, J. O., Butt, L. E., Henderson, C. A., Devonshire, M., Healy, J., Conway, S. J., Locker, N., Pickford, A. R., Vincent, H. A., and Callaghan, A. J. (2018) High-density functional-RNA arrays as a versatile platform for studying RNA-based interactions. *Nucleic Acids Res. 46*, e86.
(24) Madeira, F., Park, Y. M., Lee, J., Buso, N., Gur, T., Madhusoodanan, N., Basutkar, P., Tivey, A. R. N., Potter, S. C., Finn, R. D., and Lopez, R. (2019) The EMBL-EBI search and sequence analysis tools APIs in 2019. *Nucleic Acids Res. 47*, W636−W641.
(25) Good, L., Awasthi, S. K., Dryselius, R., Larsson, O., and Nielsen, P. E. (2001) Bactericidal antisense effects of peptide-PNA conjugates. *Nat. Biotechnol. 19*, 360−364.
(26) Goltermann, L., Yavari, N., Zhang, M., Ghosal, A., and Nielsen, P. E. (2019) PNA length restriction of antibacterial activity of peptide-PNA conjugates in *Escherichia coli* through effects of the inner membrane. *Front. Microbiol. 10*, 1032.
(27) Norouzi, M., Pickford, A. R., Butt, L. E., Vincent, H. A., and Callaghan, A. J. (2019) Application of mRNA arrays for the production of mCherry reporter-protein arrays for quantitative gene expression analysis. *ACS Synth. Biol. 8*, 207−215.
(28) Henderson, C. A., Rail, C. A., Butt, L. E., Vincent, H. A., and Callaghan, A. J. (2019) Generation of small molecule-binding RNA arrays and their application to fluorogen-binding RNA aptamers. *Methods 167*, 39−53.
(29) Imburgio, D., Rong, M., Ma, K., and McAllister, W. T. (2000) Studies of promoter recognition and start site selection by T7 RNA polymerase using a comprehensive collection of promoter variants. *Biochemistry 39*, 10419−10430.
(30) Bardill, J. P., and Hammer, B. K. (2012) Non-coding sRNAs regulate virulence in the bacterial pathogen *Vibrio cholerae*. *RNA Biol. 9*, 392−401.
(31) Rutherford, S. T., and Bassler, B. L. (2012) Bacterial quorum sensing: its role in virulence and possibilities for its control. *Cold Spring Harbor Perspect. Med. 2*, a012427.
(32) Defoirdt, T. (2018) Quorum-sensing systems as targets for antivirulence therapy. *Trends Microbiol. 26*, 313−328.
(33) Bartel, D. P. (2004) MicroRNAs: genomics, biogenesis, mechanism, and function. *Cell 116*, 281−97.
(34) Breaker, R. R. (2009) Riboswitches: from ancient gene-control systems to modern drug targets. *Future Microbiol. 4*, 771−773.
(35) Colameco, S., and Elliot, M. A. (2017) Non-coding RNAs as antibiotic targets. *Biochem. Pharmacol. 133*, 29−42.
(36) Vincent, H. A., Phillips, J. O., Henderson, C. A., Roberts, A. J., Stone, C. M., Mardle, C. E., Butt, L. E., Gowers, D. M., Pickford, A. R., and Callaghan, A. J. (2013) An improved method for the surface immobilisation of RNA: application to small non-coding RNA-mRNA pairing. *PLoS One 8*, e79142.
(37) Zuker, M. (2003) Mfold web server for nucleic acid folding and hybridization prediction. *Nucleic Acids Res. 31*, 3406−15.
(38) Gruber, A. R., Lorenz, R., Bernhart, S. H., Neuböck, R., and Hofacker, I. L. (2008) The Vienna RNA websuite. *Nucleic Acids Res. 36*, W70−W74.
(39) Lorenz, R., Bernhart, S. H., Höner Zu Siederdissen, C., Tafer, H., Flamm, C., Stadler, P. F., and Hofacker, I. L. (2011) ViennaRNA Package 2.0. *Algorithms Mol. Biol. 6*, 26.

https://doi.org/10.1021/acssynbio.0c00603
ACS Synth. Biol. 2021, 10, 1847−1858